Computer-Aided Design Optimization of High Frequency Power Inductors

Adalberto José Batista
Universidade Federal de Goiás
Escola de Engenharia Elétrica - PEQ
74605-220, Goiânia, GO – Brasil
batista@eee.ufg.br

Valério de Faria Machado
Universidade Federal de Goiás
Escola de Engenharia Elétrica - PEQ
74605-220, Goiânia, GO - Brasil
valfm@terra.com.br

***Abstract* - A computer-aided tool for design optimization of high frequency power inductors has been developed. The software uses a new optimization algorithm to design the inductor with minimum overall power loss and/or volume and to determine optimal data concerning the core and the winding. This algorithm takes full account of the current waveform and skin and proximity effects in the process of winding design optimization. The developed tool can be applied to any circuit topology provided the inductor current waveform is periodic, either with or without a dc component. An application example is given for an inductor of a 1.5 kW, 100 kHz non-resonant zero-voltage switching pulse-width modulated full-bridge dc-to-dc converter.**

I. INTRODUCTION

Several procedures for designing air-gapped inductors have been presented in the literature. These procedures present, among others, the following drawbacks: make use of empirical curves, obtained for a particular core shape and/or material, which are not readily available [1]; are limited to inductors which operate with small ac voltage components and do not account for core losses [2]; do not account for skin and proximity effects when calculating winding losses [1,2]; do not optimize the winding [1,2,3,4].

The purpose of this paper is to describe in some detail the methodology that has been developed to optimize the design of high frequency power inductors and the respective software implemented to do it. This methodology can be applied to any circuit topology provided the inductor current waveform is periodic, either with or without a dc component. By using the referred software two distinct design situations can occur and are identified as either a design limited by core loss or a design limited by core saturation. In the former, an inductor with minimum overall power loss and volume may be designed. In the latter, an inductor with minimum volume may be designed, but the overall power loss will not be minimum.

The significance of the paper is that the design procedure includes the optimization of the winding, while taking into account the current waveform and skin and proximity effects when calculating optimal data related to number of layers, conductor data, effective resistance, current density, and winding loss.

All parameters and variables in this paper are in the SI units.

II. LOSSES AND THERMAL MODELING

The design of compact and efficient magnetic components for high frequency power conversion applications, such as transformers and inductors for switched mode power supplies, requires accurate models to predict winding and core losses and the temperature of the hot spot in the component.

A. Winding Loss Model

Considerable mathematical modeling efforts carried out over the past few years have resulted in one- and two-dimensional models [5,6] to predict winding losses in such components. These models are referred to as thin layer model [5] and orthogonality model [6], respectively. A unified sense to these models appears in [7], where generalized expressions are derived for the effective resistance and leakage inductance of multilayer windings in multiwinding magnetic components under arbitrary periodic current excitation. These expressions can be applied to windings of solid round wire, bunched round wire, litz wire, or foil conductors. This reference also includes an analysis concerning the effect of winding curvature on its effective parameters and experimental data to illustrate the accuracy and the limitations of such mathematical modeling. It must be pointed out that the results obtained through the orthogonality model show that this model leads to inaccurate predictions for the effective resistance. However, the thin layer model, in spite of its simplifying assumptions, can be used as an accurate tool for design optimization purposes [8] and, for this reason, is used in the optimization methodology described here. The original thin layer model assumes that the winding structure is axisymmetric and constituted of foil conductors, which span the entire breadth of the core window. In the case of windings with solid round wire, bunched round wire, or litz wire, this model requires the replacement of the actual winding layers by equivalent-foil conductors as in the original model.

Fig. 1(a) shows a cross-section of a multiwinding magnetic component where the structure of a particular multilayer winding is detailed. According to derivations in [7], based on the thin layer model, the expression for calculating the effective resistance, R_e, of multilayer windings of foil conductors, under non-sinusoidal periodic current excitation, is given by (1). In the following equations, R_{dc} is the winding dc resistance, I_{dc} is the dc component of the current waveform, I_{ef} is the rms value of this waveform, I_{efj} is the rms value of its j'th harmonic component, f is the fundamental frequency, σ_c is the conductor conductivity and μ_o is the free space permeability. To permit calculating the winding boundary condition ratio, defined by (7), the frequency-independent magnetic field phasors between windings, caused by each harmonic component of their current waveforms, must be determined. In the case of inductors, $\bar{\varphi}_j$ is equal to zero for all j.

$$F_r = [\, I_{dc}/I_{ef}\,]^2 + \frac{1}{3}\sum_{j=1}^{\infty}[\, I_{efj}/I_{ef}\,]^2 [\, \underline{h}_j \Big/ \left|1-\bar{\varphi}_j\right|^2\,] \, x$$

$$x\{\, F_1(\underline{h}_j)[(2M^2+1)(1+\left|\bar{\varphi}_j\right|^2)+2(M^2-1)\Re(\bar{\varphi}_j)\,] +$$

$$-4F_2(\underline{h}_j)[(M^2-1)(1+\left|\bar{\varphi}_j\right|^2)+(M^2+2)\Re(\bar{\varphi}_j)\,]\} \qquad (1)$$

Where:

$$F_r = R_e/R_{dc} \qquad (2)$$

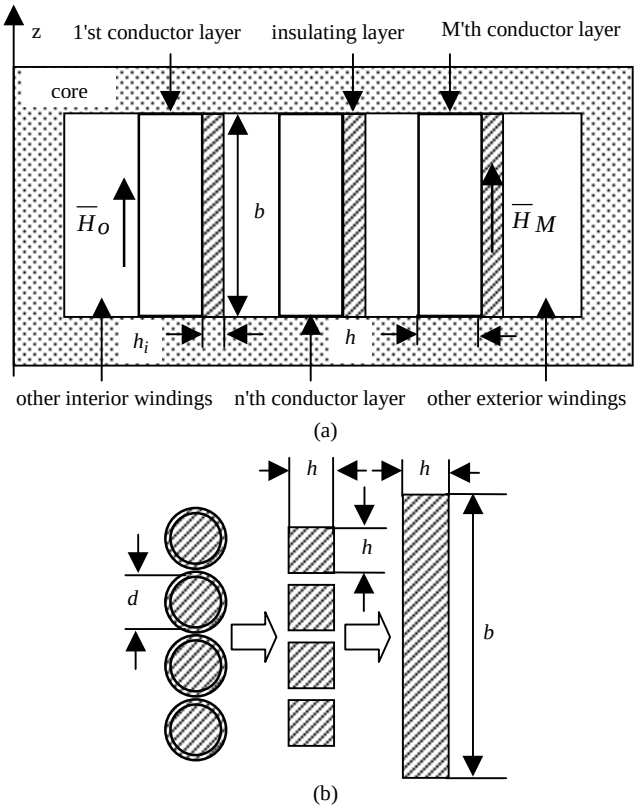

Figure 1. (a) Cross-sectional view of a multiwinding magnetic component and (b) steps to transform a layer of solid round wire into an equivalent layer of foil conductor.

$$F_1(\underline{h}_j) = \frac{senh(2\underline{h}_j) + sen(2\underline{h}_j)}{cosh(2\underline{h}_j) - cos(2\underline{h}_j)} \tag{3}$$

$$F_2(\underline{h}_j) = \frac{senh(\underline{h}_j)cos(\underline{h}_j) + cosh(\underline{h}_j)sen(\underline{h}_j)}{cosh(2\underline{h}_j) - cos(2\underline{h}_j)} \tag{4}$$

$$\underline{h}_j = h/\delta_j \tag{5}$$

$$\delta_j = \sqrt{2/j2\pi f\mu_o\sigma_c} \tag{6}$$

$$\overline{\varphi}_j = \overline{H}_{oj}/\overline{H}_{Mj} \tag{7}$$

The total winding loss is given by (8). It can be normalized by the power dissipated in the winding when $\underline{h}_1$ is equal to the unity, resulting in the normalized power given by (9).

$$P_w = R_e I_{ef}^2 \tag{8}$$

$$\underline{P}_w = F_r/\underline{h}_1 \tag{9}$$

For windings of solid round wire, the actual winding layers can be approximated by equivalent layers of foil conductor, which span the entire breadth of the core window as illustrated in Fig. 1(b) [7]. In this figure, the round conductors are replaced by square conductors of equal conducting cross-sectional area, which are brought together into a single layer foil, then stretched in order to fill the entire window breadth without changing the height of the layer. To compensate the increase in the cross-sectional area of the conducting layer, an effective conductivity $\eta\sigma_C$ is used in the field equations for the layer. The layer porosity, η, is defined as $\eta = N_b h/b$, where N_b is the number of conductor cross-sections appearing in a cross-sectional view of the winding layer, and *b* is the core window breadth. Layers of bunched round wire or litz wire are transformed similarly [7]. First, it is assumed that the total current is divided evenly among the individual strands. Second, the bunch of N_s strands with diameter d_s is replaced by a squared arrangement of $\sqrt{N_s}x\sqrt{N_s}$ conductors of equal diameter. The resultant $\sqrt{N_s}$ layers of round wire are then transformed as described previously. Therefore, for layers of bunched round wire or litz wire, whose overall diameter is D_l, N_b is given by $N_l\sqrt{N_s}$, where N_l is the number of turns per layer, and the theoretical number of winding layers, M_{wt}, is given by $M/\sqrt{N_s}$. Therefore, in the general case, the term $\underline{h}_j$ can be expressed as in (10), where *X* is given by (11).

$$\underline{h}_j = \sqrt{j}X \tag{10}$$

$$X = \sqrt{\eta}\,h/\delta_1 \tag{11}$$

Then, (1) and (9) can be expressed, generically, in terms of *X*. Figs. 2 (a) and (b) were obtained for a symmetrical triangular wave ripple current. Fig. 2(a) shows that, without a dc current superimposed on this wave, for a certain value of *M* and even for $M = 1$ there is an optimum value for *X*, which can be determined from (12), so that the normalized power is minimum. Fig. 2 (b) shows that when a dc current is present, this minimum occurs at a greater value of *X* and sufficient dc current causes the loss minima to disappear for a given *M*. In such case, the winding loss optimization will require a greater number of foil layers.

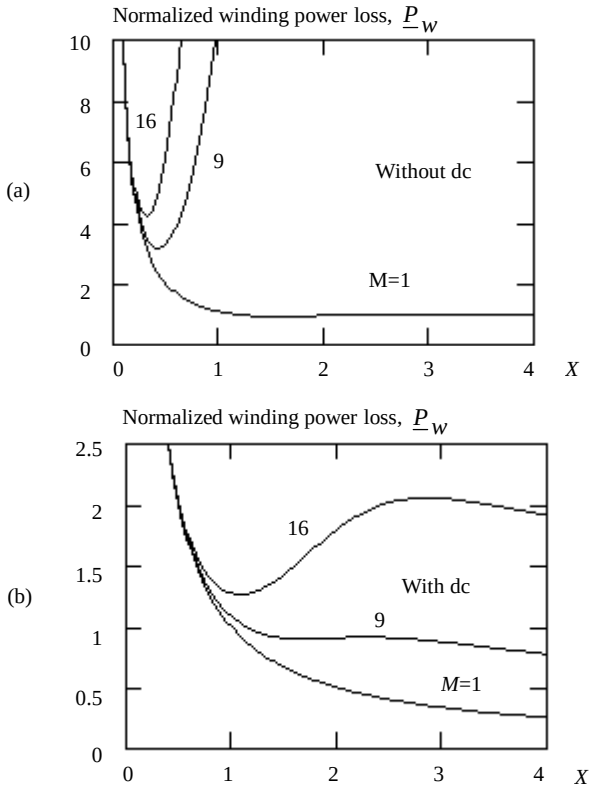

Figure 2. Normalized winding power loss as a function of the X parameter defined in (11).

$$\partial \underline{P}_w / \partial X = 0 \tag{12}$$

B. Core Loss Model

Several attempts have been made to establish a reliable method suitable for core loss measurement at high frequencies. In such measurements, the major challenge is to minimize phase errors introduced by parasitic effects in the circuit, by time delays in the coaxial cables and oscilloscope and by the digitizing process. Since a large amount of data is usually to be gathered, it is highly desirable that the measurement method used be automated in addition to being accurate and reliable. The automated measurement system for core loss characterization described in [9] can accomplish these aims within specified magnetic induction and frequency ranges and at different temperatures with high accuracy, thanks to the techniques used in the acquisition and computation of the waveforms involved in loss calculation. In this system, the measurement data are used to fit the core loss, P_c, vs. frequency, *f*, and peak-to-peak magnetic induction, ΔB, by applying the least chi-square plane method to (13), where V_e is the effective volume of the core. Some magnetic material manufacturers give the curve fitting parameters C_m, x, and y present in (13) for the respective frequency ranges in which the core loss was characterized. Some of them give the function that characterizes the dependence of C_m with temperature. However, practically no data have been published concerning core loss measurements under non-sinusoidal voltage excitation and under dc biased excitation.

$$P_c = C_m f^x (\Delta B/2)^y V_e \tag{13}$$

C. Thermal Model

The accurate modeling of the mechanisms of heat transfer is a very complex task. There are a lot of parameters that influence the thermal behavior of high frequency magnetic components. Due to this complexity, the thermal modeling requires hypotheses in order to simplify the analysis. The thermal model used at the current development stage of the software is constituted of an equivalent thermal resistance of the component, R_{th}. The relationship between this thermal resistance and the maximum overall power loss allowed in the component, P_{tm}, for a given temperature rise, ΔT, is given by (14). Some ferrite core manufacturers give the value of R_{th}, whereas others give an equation to calculate it as function of geometrical parameters. An example of such case is given in (15) [10], which was obtained by measurements on EE, EC, EFD and ETD ferrite cores. One has $k = 30.5x10^{-3}$ and $n = -0.54$ under the following conditions: full wound winding window with no layer insulation, natural convection cooling, temperature rise of 40°C, ambient temperature of 25°C, and no core losses. The fitting of this relationship with the measured results is within 20 %.

$$P_{tm} = \Delta T / R_{th} \tag{14}$$

$$R_{th} = kV_e^n \tag{15}$$

III. Optimization Methodology

A. The Basic Equations for Inductor Design

The current optimization methodology is developed under the following main assumptions: (a) the core is supposed to be operated at a magnetic induction lower than its respective saturation value, B_s, and a linear behavior is assumed for the core material; and (b) the magnetic material is supposed to have a high initial permeability and the energy is assumed to be stored in the air gap. Therefore, the following relationships, which constitute the basic equations for inductor design, can be obtained:

$$LI_p = NA_e B \tag{16}$$

$$NI_{ef} = K_u A_J J_{ef} \tag{17}$$

$$L = \mu_o \mu_e (A_e / l_e) N^2 \tag{18}$$

$$B = \sqrt{\mu_o \mu_e L / V_e}\,(I_{dc} + \Delta I/2) \tag{19}$$

$$\Delta B = \Delta I \sqrt{\mu_o \mu_e L / V_e} \tag{20}$$

$$l_g = l_e / \mu_e \tag{21}$$

In the above equations, *L* is the inductor inductance, μ_e is the relative effective permeability, *N* is the winding number of turns, I_p is the current waveform peak, ΔI is the inductor peak-to-peak current, J_{ef} is the rms value of the winding current density, A_e is the effective cross sectional area of the core, A_J is core window area, l_e is the effective magnetic core length, l_g is the overall gap length, and *B* is the peak magnetic induction. The window utilization factor, K_u, is defined by the ratio of conductive cross sectional area to the core window area and is lower than one.

The winding dc resistance is given by:

$$R_{dc} = N^2 l_t / (\sigma_c K_u A_J) \tag{22}$$

In order to take account of the fringing flux in the air gap, which increases the inductance, the desired inductance is calculated as the inductance given by (18) divided by the factor *F* given by (23).

$$F = 1 + (l_g / \sqrt{A_e}) \ln(2b / l_g) \tag{23}$$

The basic input data for designing an inductor are the following: inductance, peak and rms current, and maximum temperature rise. The design consists basically in determining the magnetic core, the air gap length, the winding number of turns and conductor data suitable to build the inductor. Suitable means that the temperature rise will not be greater than its allowed maximum value, the winding will fit into the core window, the core will not saturate and will be capable to process the required magnetic energy. This condition is mathematically expressed by (24), which can be obtained by combining (16) and (17).

$$K_u A_J A_e J_{efd} B_d \geq LI_p I_{ef} \tag{24}$$

In the above equation, J_{efd} and B_d represent the winding current density and the peak magnetic induction defined by the designer and expected to occur at actual operating conditions. How to calculate K_u, J_{efd} and B_d in order to optimize the inductor design? The answer to this question is given in the following item.

B. Optimizing the Total Loss

The inductor total loss is given by:

$$P_t = P_w + P_c \tag{25}$$

Taking into account (2), (8), (17) and (22), the winding loss can be expressed by either (26) or (27).

$$P_w = l_t K_u A_J F_r J_{ef}^2 \Big/ \sigma_c \tag{26}$$

$$P_w = l_t l_e F_r L I_{ef}^2 \Big/ (\sigma_c K_u A_J A_e \mu_o \mu_e) \tag{27}$$

Substituting the peak-to- peak magnetic induction given by (20) into (13) yields:

$$P_c = C_m f^x [(\Delta I/2)(\sqrt{L/V_e})]^y V_e (\mu_o \mu_e)^{y/2} \tag{28}$$

From (27) it should be noted that the winding loss presents an inverse dependence on the effective permeability. This originates from (18), which expresses the fact that increasing the permeability there is a tendency to reduce the number of turns, and hence to reduce the winding dc resistance. On the other hand, from (28) it should be noted that the core loss increases with increasing permeability. This originates from (20), which expresses the fact that increasing the permeability there is a tendency to increase the peak-to-peak magnetic induction. Therefore, it may be possible to optimize the inductor total loss with respect to effective permeability. Defining $(\mu_o \mu_e)_o$ to be the value at which the derivative of P_t with respect to $\mu_o \mu_e$ is zero and P_{wo} and P_{co} the resultant values for winding and core losses yields (29), which gives the optimum distribution of winding and core losses for minimum inductor loss.

$$P_{wo} = y P_{co}/2 \tag{29}$$

Combining (14), (25) and (29) yields

$$P_{wo} = (y/y+2)(\Delta T/R_{th}) \tag{30}$$

$$P_{co} = (2/y+2)(\Delta T/R_{th}) \tag{31}$$

Therefore, from (28) the following expression for the optimum effective permeability yields

$$(\mu_o \mu_e)_o = [4V_e \Big/ L(\Delta I)^2][P_{co}/(C_m f^x V_e)]^{2/y} \tag{32}$$

Now optimum values for the peak, B_o, and peak-to-peak, $(\Delta B)_o$, magnetic inductions, number of turns, N_o, current density, J_{efo}, and air gap length, l_{go}, can be obtained from (19), (20), (16), (17) and (21), respectively. However, as mentioned before, two distinct design conditions can occur. The design condition can be identified from the analysis of the dependence of the optimum peak magnetic induction on frequency. From (19) and (32) it should be noted that the peak magnetic induction increases with decreasing frequency. Therefore, there is a frequency at which the optimum peak magnetic induction is equal to the respective maximum value allowed by the designer, given by $B_m = kB_s$ (e.g., $k = 80\%$). An expression for this frequency, named transition frequency, is given by (33). If the transition frequency is lower than the current fundamental frequency, then the design is limited by core loss and the peak magnetic induction is B_o, which is lower than B_m. In this case, an inductor with minimum overall power loss and volume may be designed. On the other hand, if the transition frequency is greater than the current fundamental frequency, then the design is limited by core saturation and the peak magnetic induction is B_m. In this case, an inductor with minimum volume may be designed, but the overall power loss will not be minimum. The first step in a design procedure is to establish the design condition. The values of J_{efd} and B_d in (24) depend on this condition. In the design limited by core loss, these values are equal to J_{efo} and B_o. In the design limited by core saturation, one has $B_d = B_m$ and the winding loss is limited according to (34). Therefore, in this case, the effective permeability can be obtained from (19).

The winding effective resistance for a design limited by core loss or for a design limited by core saturation can be obtained from (30) or (34), respectively, combined with (8). Therefore, taking into account (2), (9) and (22) yields the expression for K_u given by (35). It must be pointed out that the product $X\underline{P}$ remains practically constant for *M* greater than a certain value and so does K_u.

$$f_t = [P_{co}/(C_m V_e)][2(I_{dc} + \Delta I/2)/B_m \Delta I]^{1/x} \tag{33}$$

$$P_{wm} = P_{tm} - P_c \tag{34}$$

$$K_u = l_t N^2 X \underline{P} \Big/ \sigma_c A_J R_e \tag{35}$$

Taking into account (15), (31) and (33), the following expression for the minimum effective volume that a core must have to be candidate to a design limited by core loss yields

$$V_{e\,min} = \left[\frac{2.\Delta T}{k(y+2) C_m f^x} \left(\frac{2(I_{dc} + \Delta I/2)}{B_m \Delta I} \right)^y \right]^{1/(1+n)} \tag{36}$$

This completes all expressions to compile a procedure for design optimization of high frequency inductors.

C. Optimization Procedure

The inductor optimization design algorithm was implemented by using DELPHI®. The software, which was named MAGNO, includes databases concerning conductor types and ferrite core geometries and material grades. The former file includes data about solid and bunched enamelled round copper wires and litz wires. There is also an option that allows the software to design the bunch of round wires by using solid round wires. The latter file includes all core and bobbin geometrical data, the parameters C_m, *x, y* for all frequency ranges in which the core loss was characterized, and the saturation magnetic induction. Wherever possible the parameter C_m is calculated as a function of temperature. The input data include: inductance value, core geometry and material grade, conductor type, current waveform data, ambient temperature, temperature rise and the percentage of saturation magnetic induction allowed for inductor operation. The current waveform input data include: dc component, peak and peak-to-peak current, rms current, and up to sixty harmonic components. After reading the input data, the software executes the following steps:

1. It calculates, using (36), the minimum effective volume that a core must have to be candidate to a design limited by core

loss. If there is a core of the selected type with a volume greater than this minimum, it takes this core and goes to step 3. On the contrary, it advises the designer that it is not possible to minimize the total loss by using the specified temperature rise, core geometry and material grade, and asks him/her if he/she wants to continue. If a positive answer is obtained, then it goes to step 2. On the contrary, it requires a new input data concerning temperature rise, core geometry and material grade;

2. It takes the smallest core and calculates the effective permeability, using $B = B_m$ and (19), and goes to step 4;

3. It calculates the core loss and optimum effective permeability, using (31) and (32), respectively;

4. It calculates the number of turns, using (18), rounding it to the next integer higher, and recalculates the effective permeability, using (18). If required, the correction for fringing flux is taken into account and an iterative process is used in these calculations;

5. It calculates the peak and peak-to-peak magnetic induction, core loss, air gap length, maximum overall power loss, and the maximum values to winding loss and effective resistance, using (19), (20), (13), (21), (14), (34), and (8), respectively.

6. It employs a procedure in which the number of winding layers is increased in order to get, by using the Newton-Raphson method and (12), an optimum value for *X*;

7. It calculates $\underline{P}$ by using the present values of *M* and *X*, and K_u;

8. It verifies if K_u is greater than 0.65. If it is true, it increases the number of layers, recalculates the optimum value of *X*, $\underline{P}$ and K_u until K_u converges and goes to step 9. On the contrary, it goes to step 10;

9. It verifies if K_u is in the range of 0.1 to 0.65. If it is true, it goes to step 10. On the contrary, the design proceeds with the next core of the same type and returns to either step 2 or 3, according to the design condition;

10. It calculates the dc resistance and the optimum values of *h* and N_S by using (22), (37) and (38) respectively;

11. It verifies if *M* is lower than the square root of N_S. If it is true, it increases *M*, recalculates the optimum value of *X* and returns to step 7. On the contrary, it goes to the next step;

12. It calculates the wire diameter, d_S, by using (39);

13. It selects, from the database and taking into account the conductor type and the previous calculated data, the conductor that better fits to the design. If the specified conductor type is "design bunched round wire", then the program asks for the maximum number of strands per conductor and uses this information to adjust the number of conductors in the cable, defined as a set of conductors, in order to get a total number of strands that is equal or greater than N_S and as near as possible to N_S. In this case, the design proceeds with step 14. On the contrary, it proceeds with step 15;

14. It calculates the external diameter of the cable, D_e, by using a function that depends on the number of strands per conductor and conductors per cable. This function was obtained through geometrical relationships, which were validated in practice;

15. It calculates the number of layers of the actual winding by using (40), where *B* is the bobbin height and D_e is the external diameter of the cable;

16. It verifies if the winding fits in the core window by comparing the window and the winding widths. If it does not fit in it, the design proceeds with the next core of the same type and returns to either step 2 or 3, according to the design condition. On the contrary, the design proceeds to the next step;

17. It compares the number of layers of the actual winding given by (40) with the theoretical number of winding layers, M_{wt}. If the former is greater than the latter, then it increases *M*, recalculates the optimum value of *X* and returns to step 7. If the former is lower than the latter, then the design proceeds with the next core of the same type and returns to either step 2 or 3, according to the design condition. If the former is equal to the latter, then it proceeds to the next step;

18. It recalculates the following: *h*, K_u, *X*, R_{dc}, F_r, R_e, P_w, P_t, J_{efd}, and ΔT, by using (39), (38), (37), (22), (1), (2), (8), (25), (17), and (14), respectively.

In this procedure, if there is not the referred "next core of the same type", the designer is warned and required to input new data such as temperature rise, core geometry, material type and conductor type.

$$h = bM(\delta_1 X)^2 / (K_u A_J) \tag{37}$$

$$N_S = K_u A_J / (h^2 N) \tag{38}$$

$$d_S = 2h/\sqrt{\pi} \tag{39}$$

$$M_W = N D_e / B \tag{40}$$

IV. Design Example

The application example which follows is based on a 1.5 kW, 25 A/60 V, 100 kHz zero-voltage switching pulse-width modulated and phase-shift controlled full-bridge dc-to-dc converter (FB-ZVS-PWM) [11]. In fact this converter includes an isolating transformer with a turns ratio equal to 5:1 and the current in the output filter inductor is supposed constant and equal to 25 A. Fig. 3(a) shows the basic converter power stage diagram, where the current source represents the output filter inductor current referred to the primary side of the transformer. The converter operates at a duty cycle equal to 0.9. Fig. 3(b) was obtained through a PSpice simulation and shows the current waveform in the inductor to be designed. Table I shows the main input data used for the inductor design. In all cases, the first fifteen harmonic currents was taken into account and F grade ferrite cores manufactured by Magnetics Inc. were chosen. Table II shows the curve fitting parameters of the F grade ferrite. Table III shows some of the output data that was obtained for some of the core geometries available in the MAGNO database. In this table, the cable specifications are as follow: wire gauge (AWG)/number of strands per conductor/number of conductors per cable. The option for designing "bunched round wire" was selected for all cases, but the last two ones. In these two cases the option for litz wire conductor was selected and the respective results are described in the last two lines of this table. In the present example, it was possible to design the inductor with minimum overall power loss and volume for some ferrite core and conductor types. In fact, it can be noted from the results showed in Table III and (29) that there is a "practical" optimum distribution of winding and core losses for all cases. It can also be noted that for most cases the current density results higher than its maximum commonly used value, i.e. 500 MA/m^2, and that for all cases the magnetic induction results much lower than its saturation value, i.e. 0.36 T for the F grade ferrite at 100ºC. Unlike classical design procedures, the window utilization factor is an output data. Besides, it is particularly noteworthy that the number of layers results integer, which

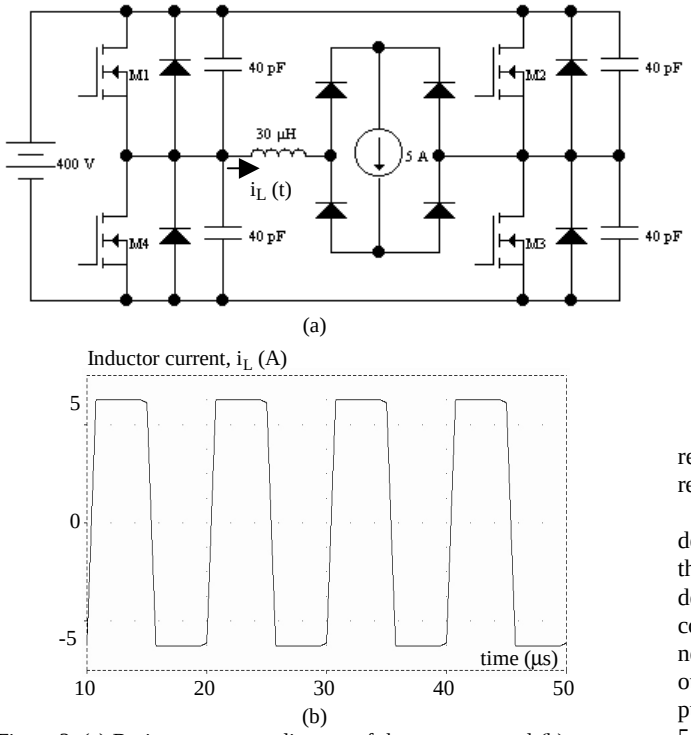

Figure 3. (a) Basic power stage diagram of the converter and (b) current waveform in the inductor to be designed.

TABLE I. MAIN INPUT DATA.

Input parameter	Value
Inductance (µH)	30
dc current (A)	0
rms current (A)	4.74
Peak current (A)	5
Peak-to-peak current (A)	10
Temperature rise (°C)	60
Ambient temperature (°C)	40

TABLE II. MANUFACTURER PARAMETERS FOR F GRADE FERRITE.

Parameter	Value
C_m (at 100°C)	0.72
x	1.66
y	2.68

results from the original purpose to design an inductor while respecting theoretical models and practical aspects.

This example shows that, by using the developed software, the designer can explore many design possibilities in order to choose the most adequate one for its application. In order to make a decision, the designer can take into account factors such as the core volume, total power loss, cost and availability of the items needed to build the inductor and easiness to build it, among others. It must be pointed out that, in each design case, the computation time has been just a few seconds on a PC Pentium III, 550 MHz and that the software retains, as default, all the data inputted and changes only new inputs.

TABLE III. MAIN OUTPUT DATA FOR SOME FERRITE CORE GEOMETRIES AND CONDUCTOR TYPES.

Core type	Core code	Effective volume (cm^3)	Winding number of		Gap length (mm)	Cable Specification	Winding Loss (W)	Core loss (W)	Temperature rise (°C)	Window Utilization factor	Current Density (MA/m^2)	Magnetic induction (mT)
			turns	layers								
EC	43517-EC	6.52	20	2	1.4393	38/18/6	1.6720	1.3538	58.28	0.1564	5.4135	87.1
EE	43009-EC	5.22	20	3	1.4007	44/19/33	1.4971	1.1709	57.92	0.3029	3.7299	89.7
ETD	43434-EC	7.80	18	2	1.3395	36/13/5	1.9310	1.4901	59.80	0.1205	5.7576	84.5
POT	43019-UG	6.12	13	2	0.9628	38/13/7	1.5318	1.1830	54.11	0.1770	6.4248	84.8
PQ	42625-UG	6.53	15	2	1.1121	37/14/5	1.6738	1.2633	56.51	0.2146	6.5993	84.9
EE	43009-UG	5.22	20	3	1.4007	44/175/4	1.4312	1.1709	56.49	0.3382	3.3409	89.7
PQ	42625-UG	6.53	15	1	1.1121	36/60/1	1.7530	1.2633	58.03	0.2271	6.2363	84.9

V. CONCLUSIONS

A new methodology to optimize the design of high frequency power inductors and the respective software implemented to do it have been described. The program searches for the smallest core that meets the design specifications and concurrently, wherever possible, it minimizes the total inductor loss. It takes full account of the current waveform and skin and proximity effects in the process of winding design optimization. In this process, it searches for the cable that better fits to the design in terms of the winding loss, number of layers, and window utilization factor. It can be applied to any circuit topology provided the inductor current waveform is periodic. An application example is given for an inductor of a 25 A/60 V, 100 kHz FB-ZVS-PWM dc-to-dc converter. Future work should concentrate on implementing an analogous methodology to optimize the design of multiwinding high frequency power transformers and on verifying the experimental validity of these theoretical designs.

VI. REFERENCES

[1] A. K. Ohri, T. G. Wilson, and H. A. Owen, "Design of Air-Gapped Magnetic-Core Inductors for Superimposed Direct and Alternating Currents", *IEEE Trans. On Magnetics*, v. Mag-12, n. 5, pp. 564-574, 1976.

[2] S. F. Szuba, "Computer-Aided Design of Air-Gapped Magnetic Core Inductors with Minimum DC Winding Resistance", *IEEE Trans. On Magnetics*, v. Mag-15, pp. 1085-1095, 1979.

[3] M. Bartoli, A. Reatti, and M. K. Kazimierczuk, "Minimum Copper and Core Losses Power Inductor Design", in *Thirty-First Anual Conference of the IEEE Industry Applications Society*, v. 3, pp. 1369-1376, 1996.

[4] Intusoft. Magnetics Designer Manual, 252 p., 1997.

[5] J. P. Vandelac and P. Ziogas, "A Novel Approach for Minimizing High Frequency Transformer Copper Losses", *IEEE Trans. On Power Electronics*, v. 3, n. 3, pp. 266-277, 1988.

[6] J. A. Ferreira, "Improved Analytical Modeling of Conductive Losses in Magnetic Components", *IEEE Trans. On Power Electronics*, v. 9, n. 1, pp. 127-131, 1994.

[7] A. J. Batista, Modelagem e Otimização do Projeto de Componentes Magnéticos Utilizados em Conversores Estáticos de Alta Freqüência, Doctoral Thesis (in portuguese), Universidade Federal de Santa Catarina, INEP, Brasil, 256 p., 1998.

[8] A. J. Batista, J. C. S. Fagundes, P. Viarouge, "Effective Resistance and Leakage Inductance in Multiwinding Transformers: Modeling, Measurement and Comparison with Numerical Solution", *in Congresso Brasileiro de Eletrônica de Potência*, pp. 731-736, 1999.

[9] A. J. Batista, J. C. S. Fagundes, P. Viarouge, "An Automated Measurement System for Core Loss Characterization", *IEEE Trans. On Instrumentation and Measurement*, v. 48, n. 2, pp. 663-667, 1999.

[10] S. A. Mulder, "On the Design of Low Profile High Frequency Transformers", in *Proc. of the HFPC*, pp. 141-159, 1990.

[11] J. L. F. Vieira; G. Gabiatti, I. Barbi, "On the Design and Experimentation of a High Performance 25 A/48 V Rectifier Unit", in *14th International Telecommunications Energy Conference*, pp. 540-547, 1992.